scientific reports

OPEN

Study on the preservation effect of ^{60}Co-γ ray irradiation on potatoes

Hao Liu[1], Zhengye Xiong[1], Qingxiang Chen[2✉], Luyan Wang[1] & Chunxi Wang[1]

To evaluate the effect of irradiation on the preservation of potatoes, fresh potatoes were selected as the irradiation objects, and irradiated with ^{60}Co-γ radiation source for 0, 100, 200, 500 and 1000 Gy, respectively. During the irradiation, the well-packaged $Y_{1.79}Bi_{0.01}Eu_{0.2}MgTiO_6$ novel thermoluminescence dosimeter material was placed together with the potatoes at the same position. Then, the potatoes were stored in the same temperature and humidity environment, and the quality changes of the potatoes were observed. The $Y_{1.79}Bi_{0.01}Eu_{0.2}MgTiO_6$ material had good performance indicators, and was used to measure the irradiation dose of the potatoes. The experiment showed that irradiation could appropriately extend the storage time of potatoes, and gamma irradiation of about 1000 Gy could achieve the best preservation effect. The main pathogenic fungi that cause dry rot of potatoes were *Fusarium solani* and *Fusarium oxysporum*, and the appropriate dose of ^{60}Co-γ irradiation could effectively inhibit the spread and growth of these fungi.

The potato (*Solanum tuberosum*) ranks as the world's fourth-largest cereal crop, with 80% of its yield suitable for human consumption[1–3]. Furthermore, potato flesh is rich in vitamins, sugars, proteins, and other essential nutrients, providing a substantial supply of nourishment for humans[4,5]. Additionally, potatoes serve as biomass energy crops and industrial raw materials[6,7]. However, during prolonged storage for sales, processing, and planting, potatoes are susceptible to contamination by dry rot, severely impacting their quality[8,9]. In China, dry rot causes approximately 10% of potato spoilage during storage, and in severe cases, this figure can reach up to 60%. Dry rot has become a significant disease during potato storage. The primary cause of potato dry rot is contamination by *Fusarium spp.*[10], resulting in decreased quality, reduced marketability, lower planting rates, and severe threats to potato safety during storage[11,12]. It is a crucial factor limiting the development of the potato industry.

Therefore, researching and developing preservation technologies for agricultural products is of paramount importance[13]. In this context, radiation preservation technology has been widely applied as an advanced new technique[14]. Different agricultural products require varying radiation doses for preservation[15], and precise control of radiation dosage is critical for radiation preservation[16]. Researching suitable thermoluminescent dosimeters (TLDs) contributes to the popularization of radiation preservation technology[17]. An ideal TLD material should possess good sensitivity[18], a wide linear range[19], stable luminescent performance under high-energy radiation excitation, a high upper dose response limit, and the ability to measure various types of radiation and ions[20,21]. Currently, several commercially available TLD materials serve different purposes: LiF[22] and $Li_2B_4O_7$: Sm[23] are suitable for personal dose monitoring, with good sensitivity but a lower linear response limit (< 50 Gy). Al_2O_3: C[24] and MgB_4O_7: Dy[25] are used for medical dose monitoring, while BeO[26], $CaSO_4$: Dy[27], and CaF_2: Ce[28] are employed for environmental dose monitoring. Although their linear response limits have improved somewhat (< 500 Gy), they have not yet reached the accurate measurement of kGy-level irradiation required for radiation preservation[29]. Other TLD materials like $CaWO_4$: Pr^{3+}[30], $SrDy_2O_4$: Eu^{3+}[31], and $BaSi_2O_5$: Dy^{3+}[32] are suitable for high-dose area monitoring, with linear response limits reaching kGy levels, albeit with suboptimal linearity.

Therefore, researching TLD materials with stable performance, high sensitivity, and a wide linear response range is crucial for radiation preservation. In this vein, the successful development of $Y_{1.79}Bi_{0.01}Eu_{0.2}MgTiO_6$ thermoluminescent dosimeter material using the high-temperature solid-phase method holds promise for radiation dose monitoring. This material can be used to study the preservation effects of potatoes under different irradiation doses and the inhibitory effects of radiation on microorganisms.

[1]School of Electronics and Information Engineering, Guangdong Ocean University, Zhanjiang 524088, Guangdong, China. [2]College of Ocean and Meteorology, Guangdong Ocean University, Zhanjiang 524088, Guangdong, China. ✉email: chenqxocean@163.com

Materials and methods
Materials and preparation

$Y_{1.79}Bi_{0.01}Eu_{0.2}MgTiO_6$ samples were prepared using the high-temperature solid-phase method. A specific amount of Y_2O_3, MgO, TiO_2, Bi_2O_3, and Eu_2O_3 (all analytical grade, purchased from Shanghai Aladdin Reagent Co., Ltd.) was weighed according to the stoichiometric ratio. The materials were ground in an agate mortar for 1 h until thoroughly mixed. Using a high-temperature alumina crucible as a carrier, the uniformly mixed material was placed in a muffle furnace for calcination. The calcination was carried out in an air atmosphere, first heating to 800 °C and holding for 3 h for pre-sintering, followed by rapid heating to 1300 °C for 9 h. After cooling to room temperature, block samples were obtained, and powdered samples were prepared by grinding in an agate mortar for subsequent use.

The potatoes were obtained from a crop planting site in Nanning, Guangxi Zhuang Autonomous Region, China, on September 26, 2023. They were individually packaged in transparent polyethylene self-sealing bags, with a total of 5 samples, each containing four potatoes, weighing approximately 900 g per sample.

Equipment and parameters

The measurement of the regeneration dose irradiation and thermoluminescence curve of the dosimeter material was performed using two instruments: Risø TL/OSL-15-B/C Thermoluminescence/Optically Stimulated Luminescence Measurement System: The irradiation source was a ^{90}Sr β radiation source with a dose rate of approximately 0.1 Gy·s^{-1}. LTTL3DS Thermoluminescence Spectrometer (produced by Guangzhou Reddy Technology Co., Ltd.): The irradiation source was an X-ray tube with an operating voltage of 50 kV and a current of 150 μA, resulting in a dose rate of approximately 0.1 Gy·s^{-1}.

Irradiation treatment

The irradiation of potatoes (including the dosimeter material) was conducted at the Guangzhou Huangpu District base of Huada Biotechnology Co., Ltd. The radiation source was a ^{60}Co-γ source with an activity of approximately 1,500,000 Ci. Prior to irradiation, 20 mg of the thermoluminescent material $Y_{1.79}Bi_{0.01}Eu_{0.2}MgTiO_6$ (already encapsulated) was placed in each potato sample. The potatoes were then irradiated for 5000, 2500, 1000, 500, and 0 s. After irradiation, the potatoes were stored at room temperature.

Results and discussion
Thermoluminescent dose response characteristics of $Y_{1.97}Bi_{0.01}Eu_{0.2}MgTiO_6$
Thermoluminescence glow curve

The thermoluminescence glow curve measurement was conducted using the Risø TL/OSL-15-B/C Thermoluminescence/Optically Stimulated Luminescence Measurement System. A sample of 20 mg $Y_{1.79}Bi_{0.01}Eu_{0.2}MgTiO_6$ powder was placed in the instrument, and the following steps were performed:

(1) Preheat the sample to 700 K and hold for 10 s.
(2) After cooling to room temperature, irradiate the sample with a ^{90}Sr β radiation source (10 Gy).
(3) Heat the sample to 700 K at a rate of 5 K/s and record the thermoluminescence glow curve.

Repeat the above steps, varying the irradiation dose to 20 Gy, 50 Gy, 60 Gy, 70 Gy, 80 Gy, 90 Gy, 100 Gy, 110 Gy, 120 Gy, 150 Gy, 300 Gy, 400 Gy, 500 Gy, 700 Gy, 800 Gy, 900 Gy, and 1,000 Gy, and measure and record the thermoluminescence glow curves. By changing the radiation source to an X-ray tube while keeping other test conditions constant, a series of X-ray irradiation thermoluminescence curves can be obtained.

To ensure reliable experimental data, the thermoluminescence was repetitively tested for different radiation sources and doses. The results showed consistent thermoluminescence curves, as depicted in Fig. 1. The curve exhibits a broad distribution extending from 350 to 700 K and features two distinct thermoluminescence peaks at temperatures of 495 K and 580 K. As the irradiation dose decreases, the shape and peak temperatures of the thermoluminescence curve remain relatively unchanged, while the thermoluminescence intensity systematically decreases[33].

Dose–response curve

To verify the relationship between thermoluminescence integral intensity and radiation dose, the integral intensity of thermoluminescence curves between 300 and 700 K at different radiation doses was determined. The resulting dose–response curve is shown in Fig. 2. Figure 2a and b represent the dose–response curves under β-ray and X-ray irradiation, respectively. Linear fits were applied to the experimental data points. Notably, neither β-ray nor X-ray irradiation exhibited saturation within the tested range. The dose response remained linear within the range of 10 to 1000 Gy, and even at 1000 Gy, a good linear relationship was maintained. This suggests that the thermoluminescent material may also exhibit a favorable linear response at higher doses. The wide linear range demonstrates the advantages of $Y_{1.79}Bi_{0.01}Eu_{0.2}MgTiO_6$ as a novel thermoluminescent dosimeter material, suitable for applications in dose monitoring[34–36]. Within the 10 Gy to 1000 Gy range, the relationship between thermoluminescence integral intensity (y) and radiation dose (x) is as follows: for β-ray excitation, $y = (2.98 \pm 0.21)*10^6 + (142.06 \pm 0.51)*10^3 \times$ and for X-ray excitation, $y = (2.96 \pm 0.36)*10^6 + (143.3 \pm 1.3)*10^3 x$. Both intercepts and slopes are consistent, and the obtained errors fall within the experimentally controllable range, requiring no further adjustments.
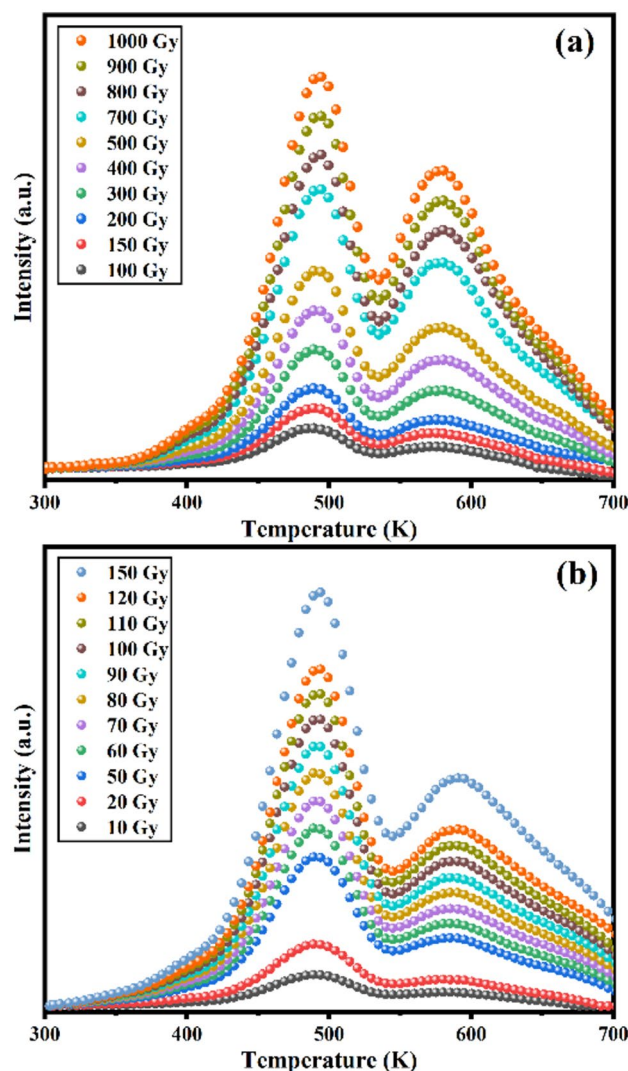
Fig. 1. Thermoluminescence curves of $Y_{1.79}Bi_{0.01}Eu_{0.2}MgTiO_6$ phosphor irradiated by a $^{90}Sr\beta$ radiation source at higher doses (**a**) and lower doses (**b**).

Dose measurement of irradiated potatoes

The dose of radiating potato was determined by analyzing the thermoluminescence (TL) curve of the pre-inserted $Y_{1.79}Bi_{0.01}Eu_{0.2}MgTiO_6$ thermoluminescent material which was pre-inserted. The TL curves were measured using a Risø TL/OSL-15-B/C thermoluminescence/optically stimulated luminescence instrument, as shown in Fig. 3a.

Remarkably, the TL curves of the material irradiated by the $^{60}Co\text{-}\gamma$ source closely resemble those obtained from β-ray irradiation. Both curves extend from 350 to 700 K and exhibit two distinct thermoluminescent emission peaks. As the irradiation time decreases, the luminescence intensity also significantly diminishes.

Based on this, calculated the integral intensity of the TL curves for irradiation times of 5000, 2500, 1000, and 500 s, resulting in values of 1.45×10^8, 7.45×10^7, 3.1×10^7, and 1.75×10^7, respectively. Using the dose–response curve, the corresponding radiation doses were determined as 999.7 ± 2.1 Gy, 499.4 ± 2.0 Gy, 198.2 ± 0.8 Gy, and 101.5 ± 1.6 Gy. These results are summarized in Fig. 3b. In subsequent observation experiments, the doses were adjusted to 1000 Gy, 500 Gy, 200 Gy and 100 Gy, respectively.

The practical utility of this thermoluminescent material was demonstrated in potato radiation preservation dose monitoring. Additionally, the radiation dose rate of the $^{60}Co\text{-}\gamma$ source was approximately 0.2 Gy/s.

Preservation effect of potatoes at different radiation doses

After $^{60}Co\text{-}\gamma$ irradiation, there were no significant changes in the morphology and quality of potatoes. Placed five groups of potatoes in a cool environment to discuss the preservation effect of potatoes under different radiation doses. The morphology of the potatoes was recorded every 5 days. The results are shown in Fig. 4.

Each column in the images represents a group of potatoes. From top to bottom, the potatoes are labeled as 1, 2, 3, and 4, and from left to right, they correspond to potatoes exposed to radiation doses of 1000 Gy, 500 Gy, 200 Gy, 100 Gy, and 0 Gy, respectively.
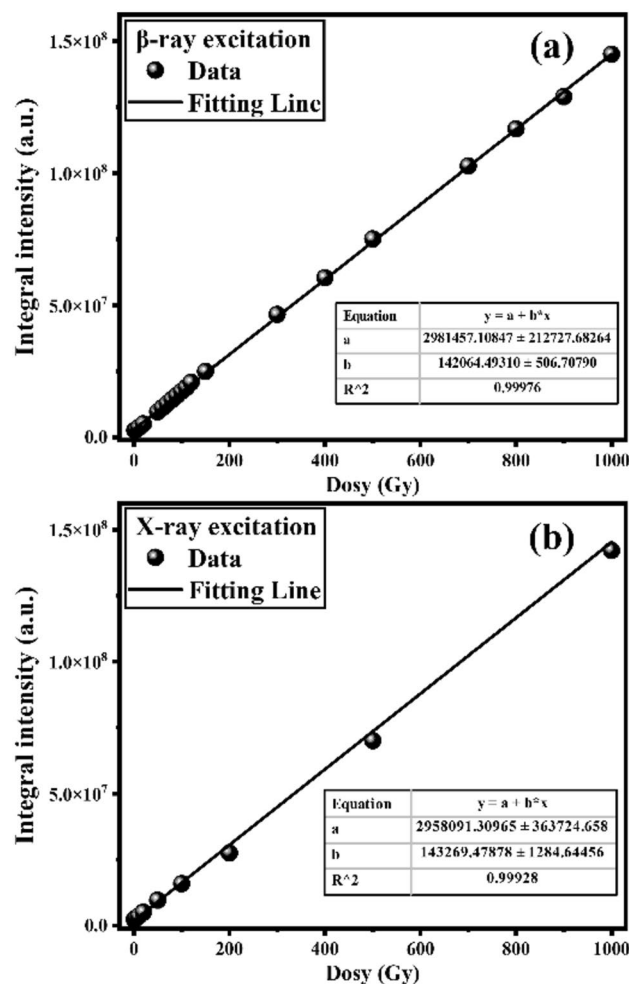
Fig. 2. Dose–response curves of $Y_{1.79}Bi_{0.01}Eu_{0.2}MgTiO_6$ phosphors under β-ray (**a**) and X-ray (**b**) irradiations.

Observations within the first 15 days revealed that the morphology of potatoes remained unchanged under different radiation doses, with no apparent signs of mold or dehydration. This study suggests that proper ultra-violet radiation does not harm pigmented potatoes and may even enhance their oxidative stress tolerance. Additionally, it increases the expression of structural genes related to anthocyanin synthesis, leading to improved yield and quality of potato tubers.

By the 20th day, noticeable changes in the morphology of potatoes occurred as storage time extended under different radiation doses. Examine the potato conditions on the 20th day, as depicted in Fig. 5:

1. Unirradiated (The fifth column):

   a. All potatoes exhibited significant mold growth.
   b. Potatoes1, 2 and 4 were visibly shriveled.

2. 100 Gy Irradiation (The fourth column):

   a. Potatoes 1 and 4 remained intact.
   b. Potato 2 experienced significant water loss.
   c. Potato 3 showed noticeable mold growth, but water loss was not severe.

3. 200 Gy, 500 Gy, and 1000 Gy Irradiation (The third column, the second column and the first column):

   a. Potatoes irradiated at these doses showed no significant changes in morphology.

   As time progressed:
   On the 25th day, the 200 Gy-irradiated Potato 1 exhibited clear mold growth.
   By the 35th day, 500 Gy-irradiated Potatoes 2 and 4 displayed evident mold growth.
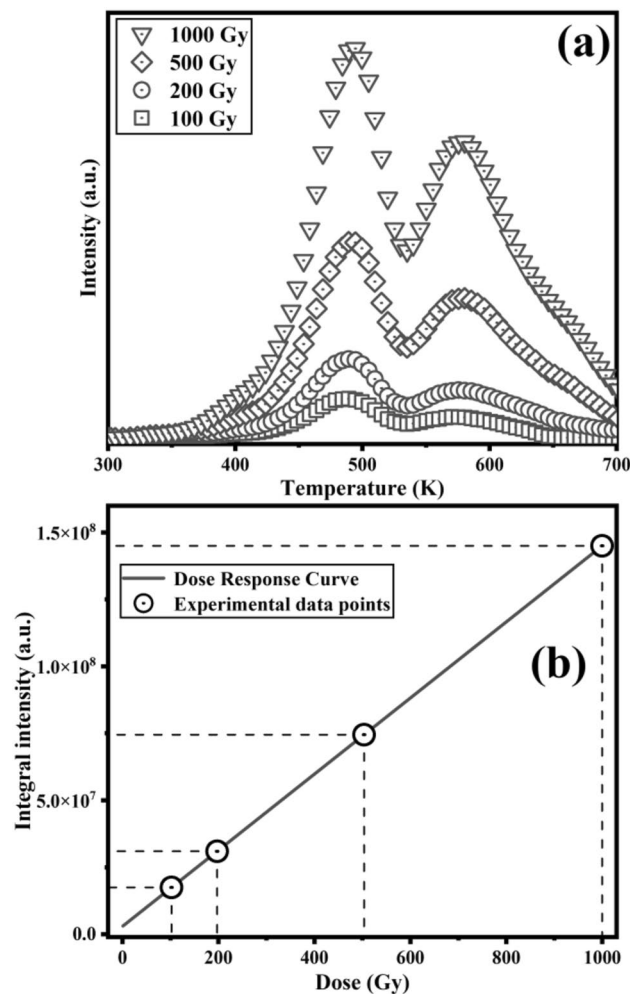   On the 40th day, the morphology of the potatoes is as shown in Fig. 6:

Fig. 3. The thermoluminescence curve (**a**) and dosimetry measurement (**b**) of different time were irradiated by ^{60}Co-γ radioactive source.

1. Unirradiated (The fifth column):

    a. All potatoes exhibit significant mold decay and severe water loss.

2. 100 Gy Irradiation (The fourth column):

    a. Potatoes 1 and 4 experience moderate water loss.
    b. Potatoes 2 and 3 show severe mold growth.

3. 200 Gy Irradiation (The third column):

    a. Potato 1 shows significant mold growth.
    b. Potatoes 2 and 3 remain intact.
    c. Potato 4 experiences moderate water loss.

4. 500 Gy Irradiation (The second column):

    a. Potatoes 1 and 3 remain intact.
    b. Potatoes 2 and 4 exhibit noticeable mold growth and severe water loss.

5. 1000 Gy Irradiation (The first column):

    a. After 40 days of storage, the potatoes show minimal change.
    b. Potato 1 has a small mold spot, and there is no evidence of water loss.

These observations provide insights into the preservation effects of different radiation doses on potatoes.

Fig. 4. Morphological changes of potato within 50 days (The time sequence is from top left to bottom right, interval of 5 days).
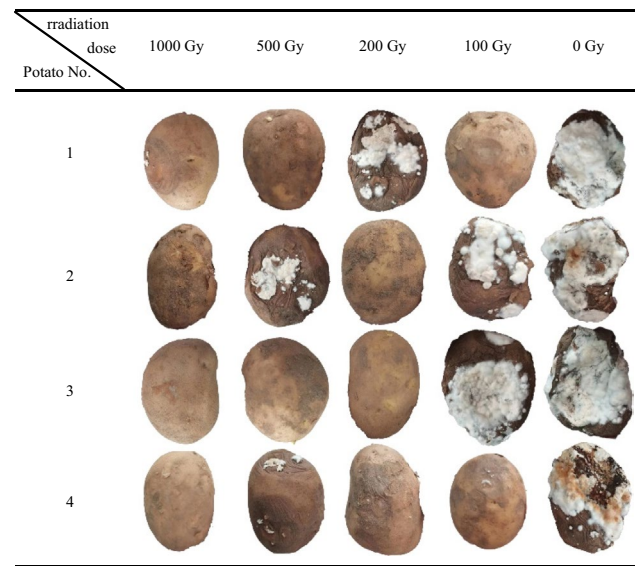

Fig. 5. Potato morphology at 20 days.

Fig. 6. Potato morphology at 40 days.

Continuing the storage until the 50th day, the moldy potatoes continued to deteriorate. To discuss the internal changes of potatoes under different radiation doses, sliced the potatoes, and the results are shown in Fig. 7:

1. Unirradiated (The fifth column):
   a. All Potatoes are severely decayed.

2. 100 Gy Irradiation (The fourth column):

   a. All Potatoes show different levels of decay.

3. 200 Gy Irradiation (The third column):
   a. Potatoes 1, 3, and 4 exhibit varying degrees of decay.
   b. Potato 2 maintains intact internal structure.

4. 500 Gy Irradiation (The second column):
   a. Potato 1 has relatively intact internal structure.
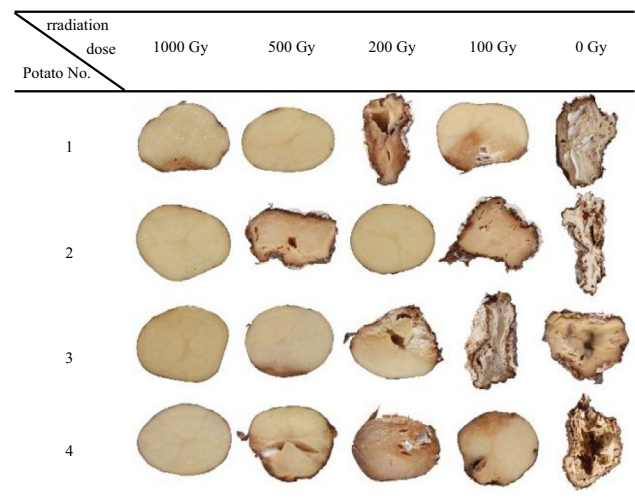   b. Potato 2 shows severe decay.

Fig. 7. Potato section at 50 days.

    c. Potato 3 experiences minor decay.
    d. Potato 4 retains good moisture but displays internal mold signs.

5. 1000 Gy Irradiation (The first column):

    a. The flesh of the potato appears healthy, with adequate moisture.
    b. Potato 1 exhibits slight decay in its flesh.

These results demonstrate that irradiation effectively prolongs potato storage. Unirradiated potatoes showed noticeable mold after 15 days, whereas irradiated potatoes delayed the onset of mold. The delay time is related to the radiation dose: higher doses lead to later mold development. At a dose of 1000 Gy, potatoes only showed mold after 40 days of storage, and by the 50th day, the mold had not significantly spread.

To investigate the cause of potato deterioration, assessed the symptoms observed during potato storage. After 15 days of storage, signs of decay became evident: localized darkening and browning of the potato skin, accompanied by increased water loss. The surface of the tubers exhibited wrinkling, indentation, and hard brown lesions. During the mid-storage period, white mycelium growth was prominent on the potatoes. In the later stages of storage, irregular concentric rings appeared within the potato flesh, leading to necrosis. Internally, the potatoes began to rot, displaying colors such as black, dark brown, light brown, or yellow–brown. These cavities were filled with white mycelium, resulting in a noticeable reduction in potato weight[37,38].

All these symptoms align with the characteristics of dry rot disease, which is the primary ailment affecting potatoes during storage[39]. Figure 8 illustrates the changes in weight and mold area of potatoes under different radiation doses during various storage periods. Notably, unirradiated potatoes suffered significant weight loss and extensive mold growth, with an approximately 80% reduction in weight after 50 days of storage. However, 1000 Gy-irradiated potatoes effectively prevented dry rot disease, maintaining weight and quality without significant changes. For potatoes irradiated at 500 Gy, 200 Gy, and 100 Gy, weight losses after 50 days of storage were 23%, 44%, and 51%, respectively.

These results demonstrate that appropriate radiation doses can partially prevent potato dry rot disease and inhibit mold proliferation, ensuring potato quality during storage.

Pathogenic fungi in potato

The primary cause of potato dry rot disease is the invasion of *Fusarium spp*[40]. To identify the specific Fusarium species, initially observed the colony morphology on potato surfaces[41]. Initially, these colonies appeared white and velvety. However, as storage time increased and mold growth occurred, the colony color gradually changed to yellow. Under a microscope at $400 \times$ magnification, examined the morphological features of their conidia (asexual spores) and conidiophores (structures that produce conidia)[42]. Based on these observations, Provisionally classified the potato strains into two categories:

Fusarium solani (Fig. 9, upper section): This type of Fusarium produces oval-shaped conidia, with numerous small conidia showing septation (division). Some large conidia exhibit a "matte" shape with rounded ends, often divided into three segments[43].

Fusarium oxysporum (Fig. 9, lower section): This Fusarium species produces elongated conidia, with most small conidia lacking septation. Large conidia have a sickle-like shape, pointed at one end[44].

To explore how fungal morphology and species change over time, further observed the potato fungi after 50 days of storage (Fig. 10). Although the number of fungi increased significantly, the species remained consistent.
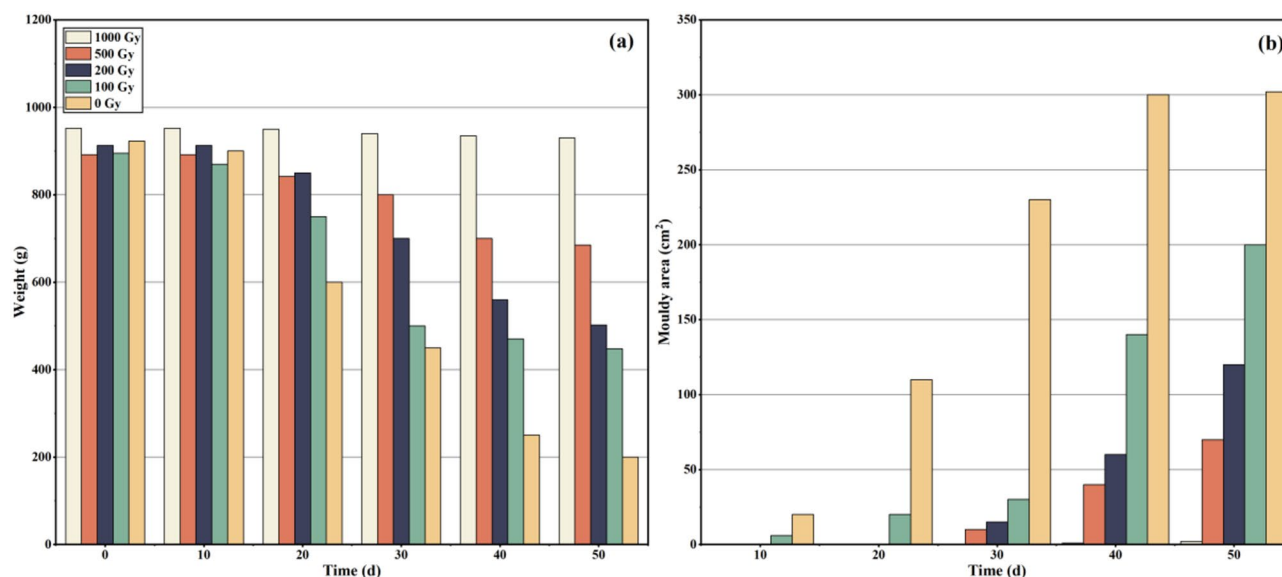

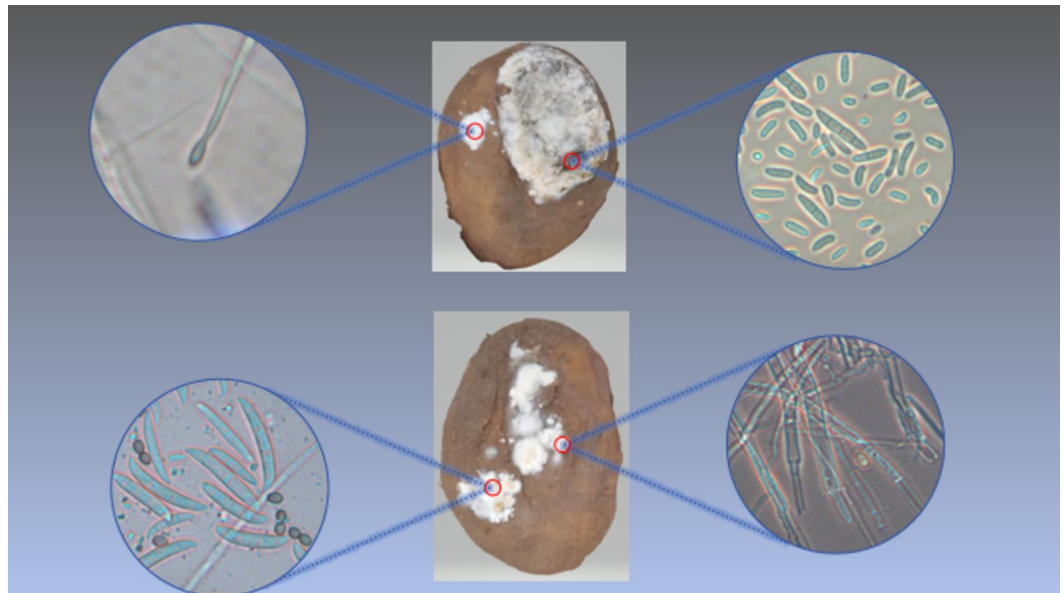**Fig. 8.** Weight (**a**) and mouldy area (**b**) of potato at different storage times.

Fig. 9. Fungal morphological characteristics of non-irradiated potato stored for 20 days.
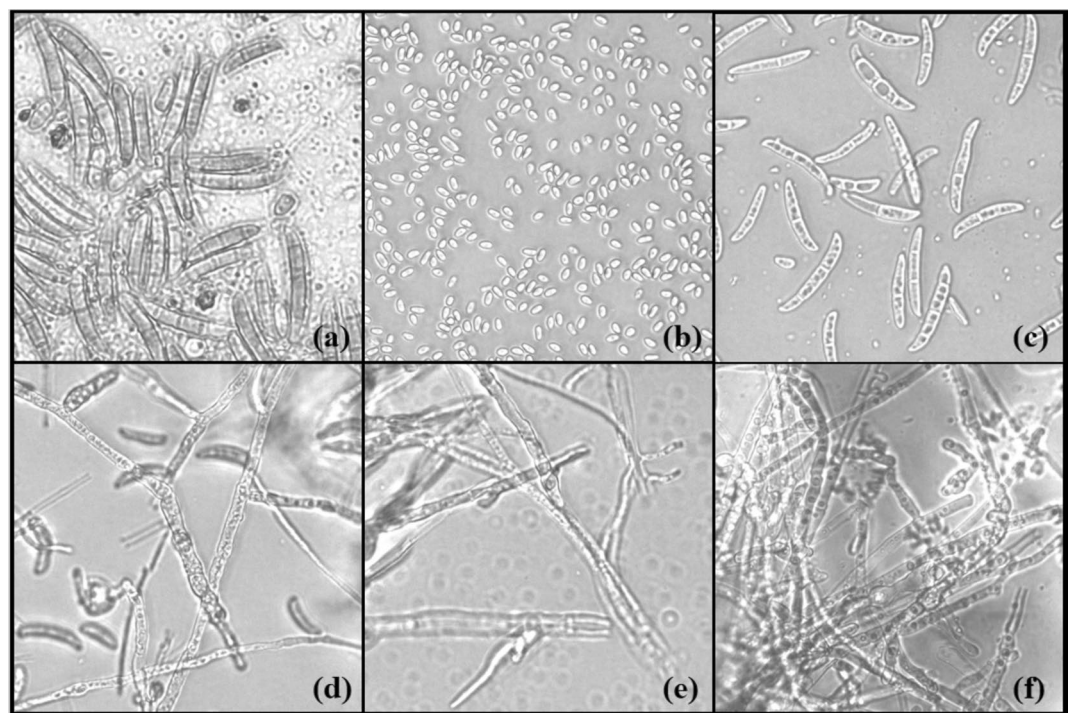

Fig. 10. Morphological characteristics of *Fusarium solani*.

The primary pathogens responsible for potato disease were still identified as Fusarium oxysporum and Fusarium solani. Notably, the fungal morphology closely resembled that observed at 20 days.

Different radiation doses mitigated the invasion and spread of these two fungi to varying degrees. Among them, 1000 Gy irradiation had the most pronounced effect. This demonstrates that radiation effectively suppresses the infection and dissemination of Fusarium solani and Fusarium oxysporum.

Conclusion

In this study, the possibility of using $Y_{1.79}Bi_{0.01}Eu_{0.2}MgTiO_6$ as a thermoluminescent dosimeter material in the field of dose monitoring was determined by evaluating the thermoluminescence curve and dose response curve of $Y_{1.79}Bi_{0.01}Eu_{0.2}MgTiO_6$ material. The thermoluminescence dosimeter material was applied to the monitoring

of potato radiation preservation dose. It was found that the storage time of potato under different irradiation doses was significantly prolonged, and the quality of potato irradiated with 1000 Gy was still good after 50 days of storage. The quality and morphology of potato will not be affected by irradiation treatment, and irradiation can effectively prevent potato dry rot and inhibit the infection and spread of *Fusarium*.

Data availability

All data generated or analysed during this study are included in this published article. The datasets used and/or analysed during the current study available from the corresponding author on reasonable request.

References

1. Aksoy, E. *et al.* Recent advances in potato (*Solanum tuberosum* L.) breeding. *Adv. Plant Breed. Strateg.* **8**, 409–487 (2021).
2. Iqbal, M. Z. & Khan, S. A. Line x Tester analysis in true seed of potato (Solanum tubersum spp tubersum). *J. Bio. Sci.* **3**(7), 674–680 (2003).
3. Deloko, D. C. *et al.* Prevalence of potato viruses on potato (*Solanum tuberosum* L.) grown in the Western Highlands of Cameroon. *J. Agric. Food Res.* **5**, 100192 (2021).
4. Singh, G. *et al.* Extracting knowledge networks from plant scientific literature: Potato tuber flesh color as an exemplary trait. *BMC Plant Biol.* **21**(1), 198 (2021).
5. Zhen, P. E. *et al.* Inheritance of steroidal glycoalkaloids in potato tuber flesh. *J. Integr. Agric.* **18**(10), 2255–2263 (2019).
6. Falter, C. *et al.* Glucanocellulosic ethanol: The undiscovered biofuel potential in energy crops and marine biomass. *Sci. Rep.* **5**(1), 13722 (2015).
7. Carlton, R. Editorial for special issue: Biomass and Energy Crops. *Food Energy Secur.* **5**(4), 210–211 (2016).
8. Baiano, A., Terracone, C., Viggiani, I., et al. Changes produced in extra-virgin olive oils from cv. Coratina during a prolonged storage treatment. Czech J. Food Sci. 32(1), (2014).
9. Hussain, S. *et al.* Benefits of rice seed priming are offset permanently by prolonged storage and the storage conditions. *Sci. Rep.* **5**(1), 8101 (2015).
10. Jiang, L. *et al.* Potential of Pantoea dispersa as an effective biocontrol agent for black rot in sweet potato. *Sci. Rep.* **9**(1), 16354 (2019).
11. Leistner, S. M. *et al.* Reduced sleep quality and depression associate with decreased quality of life in patients with pituitary adenomas. *Eur. J. Endocrinol.* **172**(6), 733–743 (2015).
12. Du, X. *et al.* Increased planting density combined with reduced nitrogen rate to achieve high yield in maize. *Sci. Rep.* **11**(1), 358 (2021).
13. Šimek, P., Vaněk, J. & Jarolímek, J. Information and communication technologies and multifunctional agri-food systems in the Czech Republic. *Plant Soil Environ.* **54**(12), 547–551 (2008).
14. Chandra, R. *et al.* Organochlorine pesticide residues in plants and their possible ecotoxicological and agri food impacts. *Sci. Rep.* **11**(1), 17841 (2021).
15. Liu, F., Chen, H. & Han, R. Different doses of the enhanced UV-B radiation effects on wheat somatic cell division. *Cell Bio.* **4**(2), 30–36 (2015).
16. Hernandez, E. A., Ferreyra, G. A. & Mac Cormack, W. P. Response of two Antarctic marine bacteria to different natural UV radiation doses and wavelengths. *Antarctic Sci.* **18**(2), 205–212 (2006).
17. Mittal, A. *et al.* Quantification of narrow band UVB radiation doses in phototherapy using diacetylene based film dosimeters. *Sci. Rep.* **11**(1), 684 (2021).
18. Liu, H. *et al.* Luminescence properties and energy-transfer behavior of $Y_{2-x-y}Bi_xEu_yMgTiO_6$ phosphors. *Heliyon* **9**(8), 2405–8440 (2023).
19. Liu, H. *et al.* Luminescence and temperature sensing properties of $Y_{2-x-y}Tm_xSm_yMgTiO6$ phosphors. *J. Lumin.* **267**, 120392 (2024).
20. Mishra, G. C., Verma, U. K., Singh, R. S. & Dhoble, S. J. Enhanced luminescence in co-doped $LaCa_4O(BO_3)_3$ phosphor: Photoluminescence, mechanoluminescence and thermoluminescence study. *Optik* **261**, 169112 (2022).
21. Donaldson, J. & Williams, G. V. M. Photoluminescence, radioluminescence, and thermoluminescence in $NaMgF_3$ activated with Ni^{2+} and Er^{3+}. *J. Lumin.* **173**, 279–285 (2016).
22. Salah, N., Sahare, P. D. & Rupasov, A. A. Thermoluminescence of nanocrystalline LiF:Mg, Cu, P. *J. Lumin.* **124**(2), 357–364 (2007).
23. Ravikumar, N. & Arun Kumar, R. Synthesis and thermoluminescence properties of $Li_2B_4O_7$: Sm phosphor for dosimetry applications. *Mater. Today Proc.* **18**(4), 1716–1723 (2019).
24. Shrestha, N., Yukihara, E. G., Cusumano, D. & Placidi, L. Al2O3: C and Al2O3:C, Mg optically stimulated luminescence 2D dosimetry applied to magnetic resonance guided radiotherapy. *Radiat. Meas.* **138**, 106439 (2020).
25. Torres-Cortés, C. O. *et al.* Synthesis and thermoluminescent response to γ-rays and neutrons of MgB4O7: Dy and MgB4O7:Dy,Na. *Appl. Radiat. Isotopes* **147**, 159–164 (2019).
26. Petrenko, M. D., Ogorodnikov, I. N. & YuIvanov, V. Thermoluminescence and low-temperature luminescence of beryllium oxide. *Radiat. Meas.* **90**, 14–17 (2016).
27. Mandlik, N. *et al.* Thermoluminescence studies of CaSO4: Dy nanophosphor for application in high dose measurements. *Appl. Radiat. Isotopes* **148**, 253–261 (2019).
28. Zahedifar, M., Sadeghi, E., Mozdianfard, M. R. & Habibi, E. Synthesis, characteristics and thermoluminescent dosimetry features of γ-irradiated Ce doped CaF_2 nanophosphor. *Appl. Radiat. Isotopes* **78**, 125–131 (2013).
29. Islam, M. S. *et al.* Impact of gamma radiation, potassium sorbate and low temperature on shrimp (Penaeus monodon) preservation. *Heliyon* **8**(12), e12596 (2022).
30. Paikaray, R. *et al.* Investigation of structural, photoluminescence, and thermoluminescence properties of Praseodymium doped $CaWO_4$ phosphor. *Mater. Today Commun.* **31**, 103802 (2022).
31. Gavhane, K. H. *et al.* Investigation of novel Eu doped $SrDy_2O_4$ microphosphor for thermoluminescence dosimetry. *J. Lumin.* **231**, 117781 (2021).
32. Alajlani, Y. & Can, N. Thermoluminescence glow curve analysis and kinetic parameters of Dy-doped $BaSi_2O_5$ phosphor. *J. Rare Earths* **40**(2), 234–242 (2022).
33. Altowyan, A. S. *et al.* Synthesis and thermoluminescence behavior of novel Sm^{3+} doped $YCa_4O (BO_3)_3$ under beta irradiation. *Ceram. Int.* https://doi.org/10.1016/j.ceramint.2024.03.089 (2024).
34. Kaur, H. *et al.* The influence of Dy^{3+} ions on physical, structural, optical, and thermoluminescence characteristics of Li_2O–BaO–B_2O_3–P_2O_5 glass system. *Mater. Res. Bull.* **169**, 112519 (2023).
35. Barad, A. *et al.* Thermoluminescence kinetics in beta-irradiated novel $ZnGa_2O_4$: Eu^{3+} phosphor produced via gel combustion synthesis. *Ceram. Int.* https://doi.org/10.1016/j.ceramint.2024.01.046 (2024).

36. Jain, M., Manju, Kumar, R. et al. Defect states and kinetic parameter analysis of ZnAl$_2$O$_4$ nanocrystals by X-ray photoelectron spectroscopy and thermoluminescence. *Sci. Rep.* 10(1):385 (2020).

37. de Sousa Santos, M. N. *et al.* Sprout-suppressing 1, 4-dimethylnaphthalene treatment reduces dry rot infection in potato tubers during postharvest storage. *Postharvest Biol. Technol.* **205**, 112485 (2023).

38. Li, Y. *et al.* The biocontrol of potato dry rot by microorganisms and bioactive substances: A review. *Physiol. Mol. Plant Pathol.* **122**, 101919 (2022).

39. Liu, Y. *et al.* Antifungal activity and mechanism of thymol against Fusarium oxysporum, a pathogen of potato dry rot, and its potential application. *Postharvest Biol. Technol.* **192**, 112025 (2022).

40. Ejaz, M. R. *et al.* An examination of how climate change could affect the future spread of Fusarium spp. around the world, using correlative models to model the changes. *Environ. Technol. Innov.* **31**, 103177 (2023).

41. Risoli, S. *et al.* Isolation and characterization of Fusarium spp. From unhatched eggs of Caretta caretta in Tuscany (Italy). *Fungal Biol.* **127**(10–11), 1321–7 (2023).

42. Rangel-Muñoz, E. J. *et al.* Presence of the toxigenic fungi Aspergillus spp. and Fusarium spp. in Musca domestica L.(Diptera: Muscidae) collected from dairy farms. *J. Dairy Sci.* **106**(8), 5468–73 (2023).

43. Huang, L. *et al.* Disseminated Fusarium solani infection in a child with acute lymphocytic leukemia: A case report and literature review. *Med. Microecol.* **18**, 100093 (2023).

44. Zhang, X. *et al.* Physiological mechanism beneath the inhibition of Cleome spinosa against the morphology and reproduction of Fusarium oxysporum. *Heliyon* **9**(12), e22622 (2023).

Acknowledgements

Author contributions

H.L. Conceptualization, Data curation, Formal analysis, Writing original draft. ZY. X. Funding acquisition, Resources, Validation. QX.C. Methodology, Supervision, review and editing. LY.W. and CX.W. Investigation.

Funding

Competing interests

The authors declare no competing interests.

Ethical approval

Study was in accordance with relevant institutional, national, and international guidelines and legislation.

Additional information

Correspondence and requests for materials should be addressed to Q.C.

Reprints and permissions information is available at www.nature.com/reprints.

Publisher's note Springer Nature remains neutral with regard to jurisdictional claims in published maps and institutional affiliations.